Noise Eliminated Ensemble Empirical Mode Decomposition for Bearing Fault Diagnosis

Atik Faysal[1], Ngui Wai Keng[2], M. H. Lim[3]

[1,2]College of Engineering, Universiti Malaysia Pahang, Lebuhraya Tun Razak, 26300, Gambang, Kuantan, Pahang, Malaysia.

[3]Institute of Noise and Vibration, Universiti Teknologi Malaysia, Jalan Sultan Yahya Petra, 54100 Kuala Lumpur, Malaysia.

Corresponding author: Ngui Wai Keng (e-mail: wkngui@ump.edu.my).

ABSTRACT

Although noise-assisted decomposition methods, ensemble empirical mode decomposition (EEMD) and complementary EEMD (CEEMD) can reduce the drawbacks of empirical mode decomposition (EMD), they cannot fully eliminate the presence of white noise. In this paper, a method named noise eliminated EEMD (NEEEMD) was proposed to reduce further the white noise in the intrinsic functions and keep the ensembles optimum. The NEEEMD algorithm also decomposes the ensemble of white noise signals using EMD and subtracts from the outputs of EEMD. A simulated signal was used to demonstrate the performance of NEEEMD using root-mean-square error (RRMSE) and time & envelope spectrum kurtosis (TESK). A sensitive mode (SM) selection method was proposed to select the most sensitive intrinsic mode functions (IMFs) from NEEEMD which takes multiplication of kurtosis in the time domain and energy-entropy in the frequency domain. Finally, to enhance the signal's fault-related impulses, an advanced filter called MOMEDA was applied to the most sensitive IMF. The significance of the proposed method was illustrated using the envelope spectrum from bearing signals containing different types of faults at various speeds and motor loads. The output of the proposed method, EEMD and CEEMD was compared using the envelope spectrum to identify fault characteristic impulses. Envelope spectrum analysis proved that our proposed method performed better in every case by providing more fault-related impulses.

KEYWORDS

Empirical mode decomposition, ensemble empirical mode decomposition, complementary ensemble empirical mode decomposition, fault diagnosis.

I. INTRODUCTION

Rotating machinery such as rolling bearings are one of the key components of the industries. Bearings and other rotating components suffer from continuous failure due to their prolonged period of operation. It is crucial to have a reliable fault diagnosis and health monitoring system to avoid any unwanted failure during operation. Tremendous research has been carried out over the past few decades, both from the industries and academia, to ensure safe operation [1].

Signal processing has been the most prominent and successful method in fault diagnosis and condition monitoring research of bearing [2][3][4]. The most effective signal processing method is the time-frequency domain analysis which includes wavelet transform [5][6], variational mode decomposition (VMD) [7][8], local mean decomposition (LMD) [9] and EMD [10] that have been employed for bearing fault diagnosis. The EMD family has been proven to be superior since it acts as a filter by producing several IMFs [11].

EMD is a popular time-frequency adaptive decomposition method that is suitable for varying and nonstationary signal analysis. EMD has gotten massive popularity in fault diagnosis and condition monitoring [12][13][14]. EMD decomposes signals into several components known as IMFs and a monotonic signal called residue [15]. Xiong et al. [16] obtained acceleration time histories from the bearing box to process them with the EMD method mixed with kurtosis criterion and noise components with signal trend were filtered. The test data was used for the validation of the proposed method which demonstrated that the system can both diagnose fault at low speed and obtain high accuracy. Song et al. [17] proposed a novel multi-layer filtering method to remove the noise and obtain weak fault features from IMFs of different layers obtained using EMD. Simulated and experimental results showed that the method can successfully filter out unwanted noise to improve accuracy.

However, one of the main limitations of EMD is the mode mixing problem described as mixing elements from different scales into one or separate IMFs. Because of this drawback,

the signal may contain some components and noise unrelated to the signal, decreasing the system accuracy. To subside the limitations of EMD, Wu and Huang [18] proposed EEMD, a noise-assisted version of EMD. EEMD adds white noise to the ensemble signals and the white noise populates the whole signal, thus drastically solves the mode mixing problem. Zou [19] applied a deep neural network to the processed signal of EEMD. The method can significantly improve fault diagnosis accuracy in case of a small sample size. Li [20] proposed a novel method to select the sensitive IMFs which was shared with advanced frequency band entropy for bearing fault diagnosis. The novel method has an advantage over other methods in terms of feature extraction. Nonetheless, to significantly reduce the presence of white noise, many ensembles are required, which increases the computational complexity.

To alleviate the drawbacks of EEMD, Yeh et al. [21] came up with CEEMD method which adds positive and negative white noise in pairs with a less ensemble number to reduce the residual noise present in the reconstructed signal. Yang [22] used a combination of wavelet threshold and CEEMD to reduce the background noise of the vibration signal from the rolling bearing. IMFs were obtained using CEEMD and selected based on kurtosis index and correlation coefficients. The fault impulses were obtained using the envelope spectrum. Lu [23] used an optimized CEEMD assisted system combined with a rigid Gaussian distribution clustering unsupervised learning algorithm for bearing fault diagnosis. The proposed model has a self-learning ability. Anyhow, CEEMD can decrease white noise to a great extent, but it does not completely eliminate the limitation and needs further attention. This paper proposes a method called NEEEMD to overcome the drawbacks of EEMD by subtracting the ensemble IMFs of noise from the ensemble IMFs of the original signal. NEEEMD reduces the drawbacks of EEMD and CEEMD within the limited number of ensembles which is validated using RRMSE and TESK.

Since the decomposition algorithms produce several IMFs and not all the IMFs have the same physical significance, it is important to identify which IMFs work further. Typically, the higher-ordered IMFs contain the most information about the signal[24]. So, it is crucial to have some method to select the most SM from the IMFs. Among many techniques proposed SM selection, He et al. [25] proposed the selection of SM by a variance regression approach. Yan and Gao [26] used both correlation measure and the energy amount to select the most SM. Lei and Zuo [27] proposed the measurement of correlation of the vibration signal and IMFs of the fault condition and correlation of the vibration signal and IMFs of the normal condition for SM selection. Wang et al. [27] proposed the selection of the IMF with the greatest value of the kurtosis index as the most SM. Nevertheless, all the proposed methods listed above are obtained from the time-domain analysis of the acquired IMFs, which overlooks the time-frequency domain characteristics of the SM. This study proposed a sensitive mode selection method that considers kurtosis in time-domain and energy-entropy in frequency-domain, thereby getting the most information out of the signal.

The noise-assisted decomposition methods can split the signal into separate modes, where the most sensitive mode contains the highest information. However, the characteristic fault impulses can be pretty low because the noise populates the entire frequency bandwidth and the white noise is present in each mode. Therefore it is required to enhance the fault impulses of the fault frequency in rotating machinery fault diagnosis. Minimum Entropy Deconvolution (MED) [28] has been used effectively by many researchers for rotating machinery fault diagnosis; however, this method has its own limitations. MED takes many iterations for the solution and, most of all, is suitable for a single impulse, whereas our signals have multiple impulses. McDonald and Zhao proposed [29] a powerful method called multipoint optimal minimum entropy deconvolution adjusted (MOMEDA) which does not require any iteration to reach the filtering solution. MOMEDA is able to extract the regular fault impact using the multipoint kurtosis in the range of the period. It has a strong versatility since it does not have to determine the fault period in advance. Zhu et al. [30] used MOMEDA to extract the bearing signal's effective components and then applied Teager energy operator (TEO) to obtain the fault features. Wang et al. [31] applied MOMEDA on simulated signal and gearbox vibration signal and effectively separated the various impact elements. In this paper, MOMEDA is applied to the most sensitive mode obtained from the IMFs after the NEEEMD decomposition. The filter's length is varied in a range to obtain the best output with maximum fault impulses from the envelope spectrum. Different bearing fault conditions at various speeds and motor loads were considered to generalize the adaptability of the proposed method. The comparison of fault impulses from the envelope spectrum demonstrates the superiority of the proposed system to individual EEMD and CEEMD.

The rest of the paper is organized as follows; Section II provides the theoretical background for all the previous methods. The proposed method was discussed in section III where the NEEEMD algorithm was validated numerically in section III.1.1. In section III.4, the summary of the proposed method was discussed. The proposed method was validated with the experimental dataset in section IV which is followed by a conclusion in the end.

II. REVIEW of EMD, EEMD, CEEMD

A. EMD

The time-frequency domain analysis EMD simply decomposes a vibration signal into several IMFs. The IMF function needs to fulfill two criteria:

1) The number of extrema and zero crossings in the whole vibration series must be the same or differ at most by one.
2) The mean of upper and lower envelopes must be zero at any given point.

When the above two criteria are satisfied, an IMF is reported by c_1. The first residue $r_1$is obtained from the difference between the signal and the first IMF and is used to decompose the next IMF. The decomposition process has to be repeated to find the nth IMF until a monotonic residue is reported. The method of decomposition is repeated n times until the residue becomes monotonic to obtain the nth IMF. The original signal can be reassembled by summing the n IMFs and the nth residue presented as follows:

$$X(t) = \sum_{i=1}^{n} c_i + r_n \quad (1)$$

where $X(t)$ is the original signal, c_i is the ith IMF, and r_n is the nth residue.

B. EEMD

EEMD is an improvement of EMD which was suggested to solve the mode fusing problem of EMD. The white noise of a finite amplitude is added with the ensembles of EMD to generate the IMFs. The added noise dissolves in the whole time-frequency plane uniformly, thus solving the mode mixing problem. For an original signal $X(t)$, the EEMD algorithm follows the following steps:

1) Add a bunch of white noise to the original signal with a mean of 0 and the standard deviation of 1 to obtain a series of ensembles.
$$X_i(t) = X(t) + w_i(t) \quad (2)$$
Where $w_i(t)$ is the white noise signal of the same length as $x(t)$ and $i = 1,2, \dots, M$, M is the number of ensembles.
2) Decompose the ensembles using EMD to obtain the IMFs.
$$X_i(t) = \sum_{j=1}^{N} c_{ij}(t) + r_i(t) \quad (3)$$
Where $j = 1,2, \dots, N$, N is the number of IMFs and $c_{ij}(t)$ is the IMFs $(c_{i1}, c_{i2}, \dots, c_{iN})$. $r_i(t)$ denotes the residue of the ith trail.
3) In the end, determine the ensemble means of the consequent IMFs.
$$c_j(t) = \frac{1}{M}\sum_{i=1}^{M} c_{ij}(t) \quad (4)$$

C. CEEMD

CEEMD was proposed to overcome the drawbacks and increase the performance of EEMD. In CEEMD, white noise is added in pairs (both positive and negative) to reduce the presence of noise. The paired white noises can decrease the white noise in the final residue successfully. The CEEMD algorithm for a signal $X(t)$ has the following steps:

1) Add a pair of white noise to $x(t)$ the same way as EEMD.
$$X_1(t) = X(t) + w_i(t) \quad (5)$$
$$X_2(t) = X(t) - w_i(t) \quad (6)$$
2) Decompose $X_1(t)$ and $X_2(t)$ using EMD to obtain the IMFs.
3) Obtain two ensemble IMFs sets by repeating the steps M times.
$$IMF_1 = \frac{1}{M}\sum_{i=1}^{M} IMF_{1i} \quad (7)$$
$$IMF_2 = \frac{1}{M}\sum_{i=1}^{M} IMF_{2i} \quad (8)$$
4) The final IMFs are obtained from the mean of positive and negative ensembles.
$$IMF = (IMF_1 + IMF_2)/2 \quad (9)$$
5) The final result is obtained as,
$$X(t) = \sum_{i=1}^{M} IMF_i(t) + r_M(t) \quad (10)$$

III. PROPOSED METHOD

A. NEEEMD

The NEEMD takes a different approach than CEEMD to eliminate the white noise in the final stage. Instead of adding a negative white noise at the primary stage, it subtracts the IMFs of the same white noise from the final IMFs. The steps of NEEEMD are followings and also illustrated in Fig. 1.

1) Add ensemble of white noise $w_i(t)$ (whose length is the same as the original signal with a mean of 0 and the standard deviation of 1) to the original signal $X(t)$ and obtain $X_i(t)$.
2) Follow the steps from equation (2) to (4) to obtain the ensemble means of the IMFs, $c_j(t)$.
3) Take out the input ensemble white noise $w_i(t)$ and apply EMD to it.
$$W_i = \sum_{j=1}^{N} wc_{ij}(t) + wr_i(t) \quad (11)$$
Where $j = 1,2, \dots, N$, N is the number of IMFs and $wc_{ij}(t)$ is the IMFs of noise $(c_{i1}, c_{i2}, \dots, c_{iN})$. $wr_i(t)$ denotes the residue of the ith trail.
4) Compute the ensemble means of the IMFs for the white noise.
$$wc_j(t) = \frac{1}{M}\sum_{i=1}^{M} wc_{ij}(t) \quad (12)$$
5) Subtract the IMFs of noise from the IMFs obtained from EEMD for the reduction of white noise.
$$IMF_j = c_j(t) - wc_j(t) \quad (13)$$
6) The original signal can be obtained such that,
$$X(t) = \sum_{i=1}^{M} IMF_{ij}(t) + r_{Mj}(t) - wr_{Mj}(t) \quad (14)$$

Where $wr_M(t)$ is the residue of the white noise.

1) Numerical Validation

The NEEEMD method is validated by comparing with EEMD and CEEMD using a simulated signal. The simulated

signal $X(n)$ consists of three components which are a continuous absolute tone plus a gapped one, namely, $X_1(n)$, $X_2(n)$ and $X_3(n)$, where they have a greater frequency, cosine signal, and a quadratic trend, respectively.

$$X(n) = X_1(n) + X_2(n) + X_3(n) \tag{15}$$

$$X_1(n) = \begin{cases} 0, \\ \sin\big(2\pi \times 0.3(n-501)\big), \\ 0, \end{cases} \quad \begin{matrix} if\ 1 \le n \le 500 \\ if\ 501 \le n \le 750 \\ if\ 751 \le n \le 1000 \end{matrix} \tag{16}$$

$$X_2(n) = \cos\big(2\pi \times 0.05(n-1)\big) \tag{17}$$

$$X_3(n) = \frac{n}{1000} + \left(\frac{n}{1000}\right)^2 \tag{18}$$

The simulated signal equation is adopted from [32] where the first two signals represent the classical mode-mixing problem and the last one is the frequently used quadratic trend in the signal model. The three-component signals and the combination of them in the time-domain waveforms are plotted in Fig. 2.

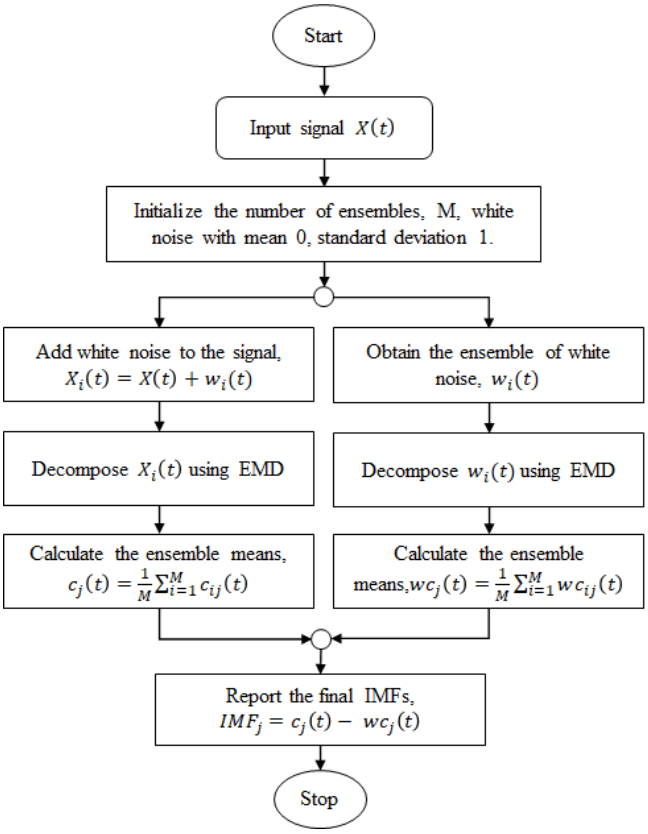

FIGURE 1. Flow chart of NEEEMD steps.

First, EMD is applied to the simulated signal to observe the effect since all the undertaken methods use EMD for processing. The EMD algorithm stops for a maximum of 4 iterations and obtains 4 IMFs and 1 residual. Since it is well established that the higher-order IMFs possess more information, the first four IMFs would be sufficient for consideration for all the methods, i.e. EEMD, CEEMD and NEEEMD. For the selection of white noise parameters for a well-established method was provided by Wu and Huang [33] to manage added white noise effect:

$$\varepsilon_m = \frac{\varepsilon}{\sqrt{M}} \tag{19}$$

Where, ε is the white noise amplitude, M is the number of ensembles and ε_m is the standard deviation of the error characterised as the difference between the input data and the consequent IMFs. Unfortunately, no solid support has been provided in the previous studies so far to select the best amplitude of the added white noise. However, some earlier works took the number of ensembles as a few hundred and the combined white noise with an amplitude of 0.2 times the standard deviation of the main signal which led to satisfactory result [34]. The number of ensembles in this research is 100 and the standard deviation of the white noise is 1 and the mean of it is 0.

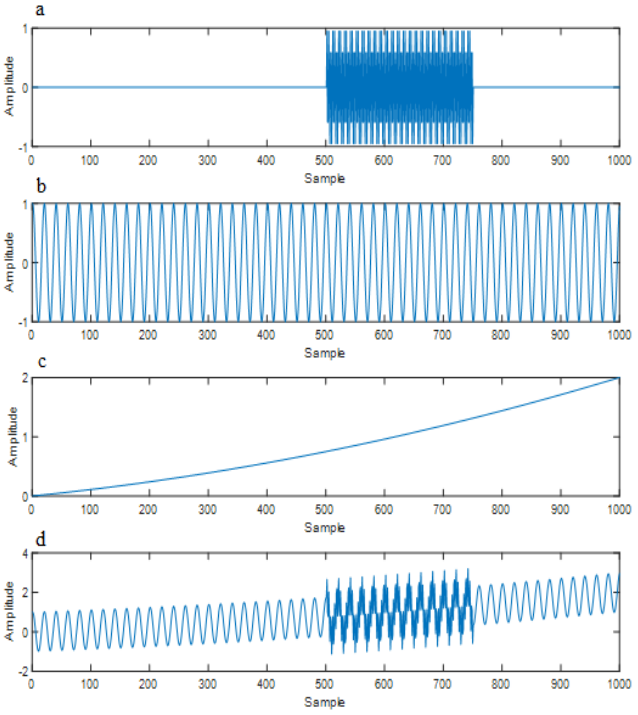

FIGURE 2. Time-domain waveform signals of: (a) $X_1(n)$; (b) $X_2(n)$; (c) $X_3(n)$; (d) $X(n)$.

The EEMD and CEEMD algorithms deal with the ensemble white noise and have been well established to perform better than the original EMD. Since this study tries to overcome the limitations of EEMD and CEEMD, any further analysis on EMD is not conducted. So, the decomposition results from EEMD, CEEMD and NEEEMD are presented in Fig. 3.

Although the EEMD and CEEMD algorithms solve the mode mixing problem greatly, from Fig. 3, it is observed that the problem is present in the later IMFs, such as in IMF3 and IMF4. This means that the mode mixing phenomenon was avoided in the earlier stages but became apparent in the later

stages. In IMF3 of EEMD and CEEMD at the sample region around 500 to 750, it is clearly affected by the mode from IMF1. On the other hand, the mode is much less present in the IMF3 of NEEEMD. Moreover, the IMF4 of EEMD is affected by mode mixing problem from the beginning to up until around 450 of the sample points. However, this problem was not present in the IMF4 of CEEMD and NEEEMD.

To emphasise the effect of the proposed method further, a frequently used evaluation parameter, RRMSE, is implemented to calculate the restoration error. The ratio between the root-mean-square of the main and reference signal, $(a-b)$ and the root-mean-square of the reference signal, b is defined as RRMSE [35] and presented as follows:

$$RRMSE = \frac{\|a-b\|}{b} \tag{20}$$

Here, the rebuilt signal means the sum of all the IMFs and residual. The value of RRMSE for all the methods is listed in Table 1. The result shows that the RRMSE value for the proposed method in this study is considerably better than the previous methods; 0.1126 for EEMD, slightly reduced for CEEMD, 0.1099, and significantly reduced for NEEEMD, 0.0143. This indicates that the NEEEMD algorithm contains the least error in the reconstructed signal than the EEMD and CEEMD methods.

The kurtosis value is an excellent parameter for measuring the signal strength and calculating how much information the signal carries. Wang et al. [13] used the multiplication of the kurtosis in the time and the envelope spectrum domain which can be applied to determine the strength of the signal. The method is called TESK and is defined as:

$$tk = k_c . k_{es} \tag{21}$$

Where,

$$k_c = \frac{E(x(t)-\mu_c)^4}{\sigma_c^4} \tag{22}$$

$$k_{es} = \frac{E(es(f)-\mu_{es})^4}{\sigma_{es}^4} \tag{23}$$

with $x(t)$ as the IMF to be analysed, σ_c as the standard deviation of $x(t)$, μ_c as the mean of $x(t)$, $es(f)$ as the envelope power spectrum of $x(t)$, μ_{es} as the mean of $es(f)$, μ_{es} as the standard deviation of $es(f)$ and $E(.)$ as the expectation operator.

The higher the tk value, the more information the signal contains. So, the total value of tk from different signals can be compared to determine the performance of the algorithms. For comparing the effectiveness of different methods, the tk values from the original signal, noise-assisted methods and the proposed method were presented in Fig. 4. The tk values for the EEMD, CEEMD and NEEEMD are 771.62, 839.39 and 905.97, respectively. It is noticed that the proposed method has the highest tk value and thus verifies the efficacy of the recommended method.

2) Selection of the SM

Another important criterion of the decomposition method is the selection of the SM. The fault information primarily happens mostly in the most sensitive IMF. Moreover, if the positions of the most SM can be selected, further decomposition can be stopped immediately to reduce the computational burden. Thus, it is necessary to locate the SM for further study automatically. This paper focuses on identifying the most SM from each trail that contains the highest fault information. Therefore, the selection procedure is conducted after obtaining the IMFs to locate the most representative SM.

In most of the previously conducted studies, the selection of the SM with the combination of the time-frequency domain has been ignored. Only a first few IMFs generally contain the fault-related information of the vibration signals. For the fault in different components of rolling elements, the frequency pattern of the vibration signals also changes along with the energy of the fault signals [36]. The baseline condition's energy distribution is commonly even and stable and thus varies from the fault signal. Hence, the energy-entropy pattern can be analyzed to specify whether the component has faults. Kurtosis has been widely used to choose the IMFs, including the highest information, as it is susceptible to the effects of faults. A high impulse signal has a larger kurtosis value, whereas a flat signal with little variation has a lower kurtosis value. This paper fuses kurtosis in the time-domain and energy-entropy in the frequency-domain to consider both time-domain and frequency-domain for SM selection.

The equation for the kurtosis of the sub-band is provided below:

$$K_j^m = \frac{\sum\{[x_j^m(t)-\overline{x}_j^m(t)]^4\}}{\sigma_{x_i^m(t)}^4} \tag{24}$$

The following stages give the process of calculation for the energy-entropy of IMFs:

1) Compute the ith IMF energy

$$E_i = \sum_{j=1}^{m} |c_{ij}|^2 \tag{25}$$

where m is the length of an IMF.

2) Compute the total energy of these n obtained IMFs

$$E = \sum_{i=1}^{n} E_i \tag{26}$$

3) Obtain the total energy-entropy of these IMFs

$$H_{en} = -\sum_{j=1}^{n} p_i \log(p_i) \tag{27}$$

where H_{en} is the energy-entropy computed from the whole original signal and $p_i = E_i/E$, is the ratio of the energy of the ith IMF relative to the whole energy-entropy.

Finally, the most sensitive IMF is obtained by multiplying kurtosis and energy-entropy value.

$$SM = K_j^m . H_{en} \tag{28}$$

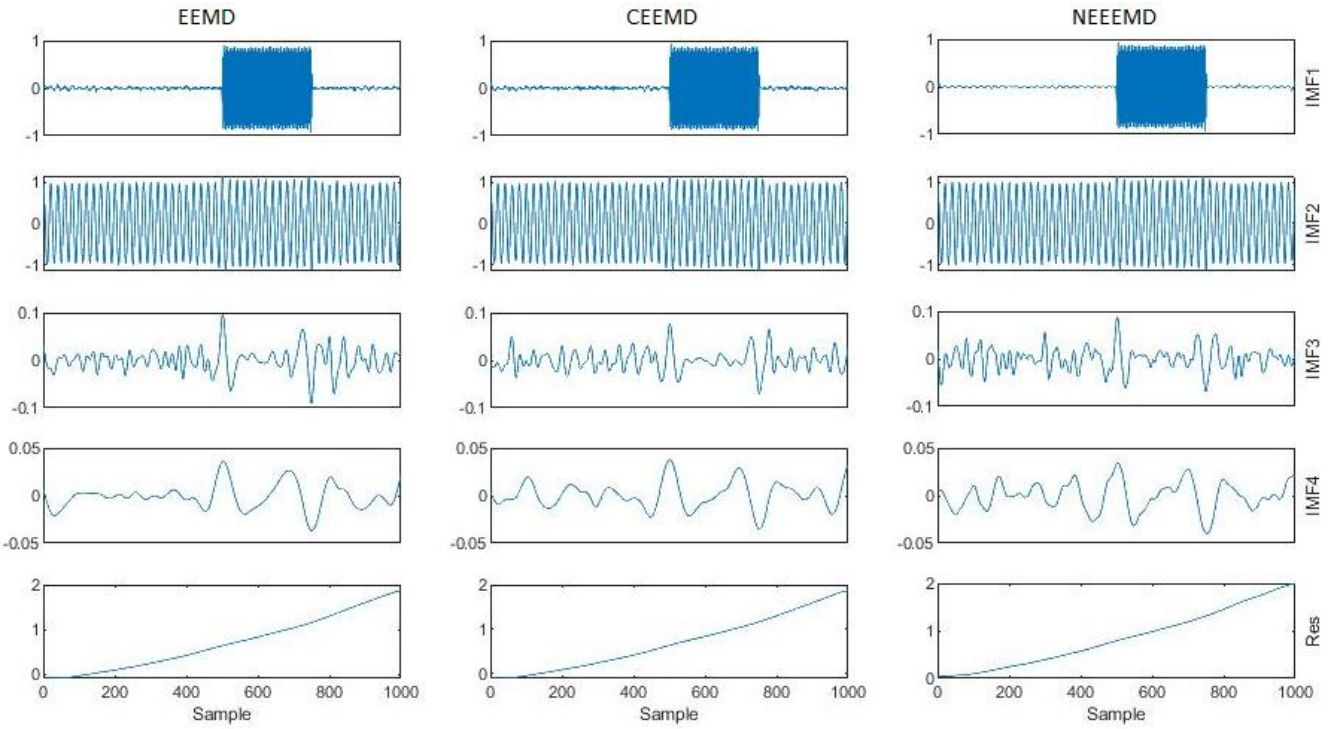

FIGURE 3. Decomposition result of the simulated signal using EEMD, CEEMD and NEEEMD, respectively.

TABLE 1. The RRMSE value of EEMD, CEEMD and NEEEMD.

	EEMD	CEEMD	NEEEMD
RRMSE	0.1126	0.1099	0.0143

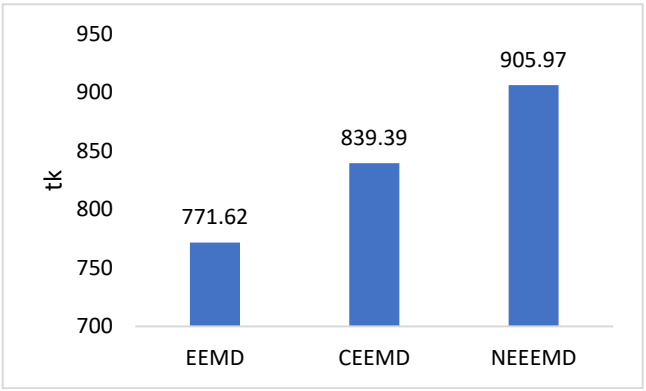

FIGURE 4. tk value obtained from the undertaken decomposition methods.

2.1) Comparison with Others SM Selection

Our proposed SM selection method using kurtosis and energy-entropy value is compared with other methods in the bearing fault diagnosis field to show superiority. As explained in the literature, we considered the previous methods that use correlation [26], kurtosis [27], and variance [25] with our proposed one. Since the goal is to select only one IMF, we tried to establish how low the other IMFs are from the selected IMF in value. A random sample from a random fault condition was obtained for this experiment. All the SM values are normalized between 0 to 1 for a fair comparison on a similar scale. The results (Fig. 5) show that our proposed method has the highest difference between the selected IMF and the next most sensitive IMF. So, it can be concluded that the proposed SM method performs better than the previous methods.

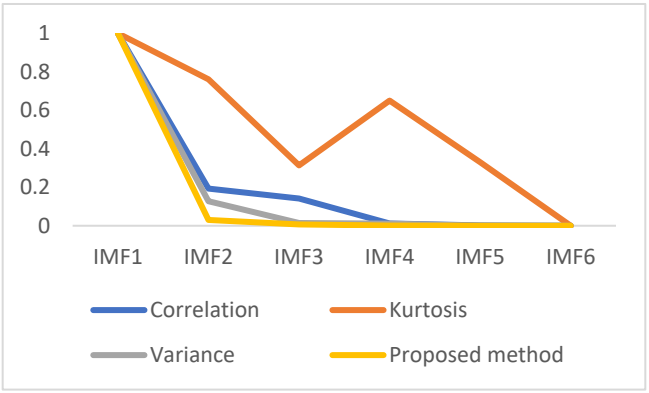

FIGURE 5. Obtained SM values from the IMFs using different mode selection methods.

3) MOMEDA

The main advantage of MOMEDA [29] over the previous methods is it can obtain multiple fault-related impulses from the vibration signal using no iteration. It proposes a straightforward solution to the optimal filter using a deconvolution method with an indefinite impulse train. A

target vector in MOMEDA represents the weightings and location of the impulses for deconvolution. Thus, it allows the regular impulse to train target goals of deconvolution that are well-fitted to the fault types of rotating machines of a single impulse-like vibration source of each rotation. MOMEDA does not require any iteration for the filter selection as it has an optimal solution with no iteration which is direct for the filter. The target vector sets can be solved simultaneously, which allows the spectrums of faulty versus period analyzed to plot accordingly. Thus, MOMEDA can further increase the fault-related periodic impulses further from the input signal and obtain a more precise filtered output.

In the resonant frequency spectrum, the impact of fault is modulated and widely distributed. This fault characteristic can be found as a regular peak distributed in the resonance spectrum band. MOMEDA designs the optimal filter for obtaining the fault-related frequency and takes the kurtosis measurement as the index to diagnose the fault characteristics of the rotating machinery. The acquired signal can be presented as:

$$y(n) = h(n)x(n) + e(n) \tag{29}$$

where $h(n)$ is the transfer function, and $e(n)$ is the noise signal and $x(n)$ is the shock signal.

MOMEDA tries to construct a filter to obtain the fault impulses from the original signal.

The steps of the MOMEDA process is listed as follows:

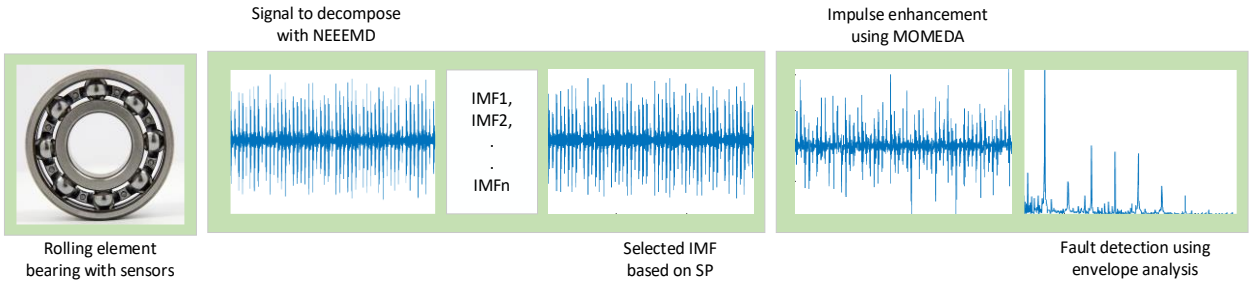

FIGURE 6. Complete steps for fault diagnosis using the proposed method.

Table 2. Characteristics of fault frequency for different fault conditions at various speed.

Fault Case	Fault type	Fault diameter	Load	Rotating frequency	Characteristics frequency	Fault frequency
Case 1	Inner race fault, f_i	0.007”	0 hp	29.95 Hz	5.415	162.179 Hz
Case 2	Ball Fault, f_b	0.014”	1 hp	29.53 Hz	4.714	139.204 Hz
Case 3	Outer race fault, f_o	0.021”	3 hp	28.83 Hz	3.585	103.368 Hz

Step 1: First, the MOMEDA equation

$$\text{Multi D} - \text{Norm} = MDN(y,t) = \frac{1}{\|t\|}\frac{t^T y}{\|y\|} \tag{30}$$

$$\max_f MDN(y,t) = \max_f \frac{t^T y}{\|y\|} \tag{31}$$

where t is a deconvoluted pulse constant vector which defines the weight and position of the target.

Step 2: Obtain the highest value from the formula above to get the optimal filter f for the pulse t;

$$\frac{d}{d_f}\left(\frac{ty}{\|y\|}\right) = \frac{d}{d_f}\frac{t_1 y_1}{\|y\|} + \frac{d}{d_f}\frac{t_2 y_2}{\|y\|} + \cdots + \frac{d}{d_f}\frac{t_{N-L} y_{N-L}}{\|y\|} \tag{32}$$

$$M_k = \begin{vmatrix} x_{k+L-1} \\ x_{k+L-2} \\ \vdots \\ x_k \end{vmatrix} \tag{33}$$

Then the formula can be written as

$$\frac{d}{d_f}\left(\frac{t_k y_k}{\|y\|}\right) = \|y\|^{-1}(t_1 M_1 + t_2 M_2 + \cdots + t_{N-L} M_{N-L}) - \|y\|^{-3} t y X_0 y \tag{34}$$

Simplify the above formula

$$t_1 M_1 + t_2 M_2 + \cdots + t_{N-L} M_{N-L} = X_0 t \tag{35}$$

Solve the highest value of the above formula

$$\|y\|^{-1} X_0 t - \|y\|^{-3} t y X_0 y = 0 \tag{36}$$

$$\frac{ty}{\|y\|^2} X_0 y = X_0 t \tag{37}$$

$$\frac{ty}{\|y\|^2} f = (X_0 X_0^T)^{-1} X_0 t \tag{38}$$

The multiple of f can be expressed as follows which is the solution of the given formula too:

$$f = (X_0 X_0^T)^{-1} X_0 t \tag{39}$$

Where,

$$X_0 = \begin{vmatrix} x_L & x_{L+1} & x_{L+2} & \cdots & x_N \\ x_{L-1} & x_L & x_{L+1} & \cdots & x_{N-1} \\ x_{L-2} & x_{L-1} & x_L & \cdots & x_{N-2} \\ \vdots & \vdots & \vdots & \ddots & \vdots \\ x_1 & x_2 & x_3 & \cdots & x_{N-L+1} \end{vmatrix} \quad (40)$$

Step 3: Obtain the reconstructed signal's kurtosis value corresponding to each t in the range by setting the search interval range R.

Step 4: Based on the kurtosis spectrum, obtain the pulse constant t related to the maximum kurtosis value.

3.1) Selection of MOMEDA Parameters

MOMEDA has several deconvoluted parameters, including the filter length L, window function w, and fault period range $[T_i, T_f]$. Appropriate tuning of the input parameters is important for improved MOMEDA performance.

1) To develop the target vector, a window function w is applied. Thus, the spectral clarity increases and the accuracy of extracted fault characteristic impulses is increased [37]. Considering the filtering effect and computing efficiency, a rectangular window of length 3 is adopted in this study.
2) The extraction result of the fault impulse sequence is directly affected by the filter length, L. L needs to be satisfied to ensure that the obtained impulse signal can comprise the whole frequency range of the fault signal [38].

$$L > 2f_s/f_c \quad (41)$$

Where f_s denotes the sampling frequency of the primary signal, and f_s represents the characteristic fault frequency. However, as the filter length increase, the sequence of fault impulse output is also reduced to $(N - L + 1)$, which leads to the fault information loss after deconvolution. On the other hand, it also takes a longer computing time. Therefore, a grid search strategy was applied within a range of filter length 10 to 50 [37] in this paper.

The search range of fault period $[T_i, T_f]$, where, T_i and T_f are the initial and final values of the search range of fault period, respectively. With respect to the rotational speed and the computation equations of fault frequency, the fault impulses of the respective components can be obtained. In the real world, the operating speed of the rotating machine will vary in a specific limit. So, the real fault frequency may differ from the theoretical value. Considering that, during the extraction of different fault impact components, the periodic initial value T_i is selected as 5. Reference [39] has verified that the extraction result of the fault impact signal will not be affected by the periodic final value T_f. In this study, the periodic final value $T_f = 300$ is espoused for all fault cases as motivated from [39].

4) Summary of the Proposed Method

When defects occur on rotating machinery, the information of fault in the signal is represented as a sequence of regular impulses. As the machinery is generally surrounded by intense noise and various external interference from the nearby machines, the reference signal is accompanied by fault impulses, random impulse components from the environment and other discrete harmonic signals from various components. Thus, the fault impulses emerge with obscurity in the raw vibration signal which makes it difficult for identification. For an effective fault diagnosis system, the fault impulses must be extracted from the raw signal. The numerical validation of NEEEMD already demonstrated that it is more effective than EEMD and CEEMD in terms of white noise and reduced reconstruction error. Therefore, NEEEMD can effectively separate the modes from the signal components. However, only the higher-order IMFs contain the most information on the fault condition. So the selection of the most SM can be conducted with the proposed SM method. Moreover, since the white noise combined with the raw data populates the entire frequency bandwidth, each mode inescapably holds some sort of noise. This white noise condition makes it hard to extrapolate the fault-related information. So, the fault impulses in the modes need to be enhanced for successive analysis.

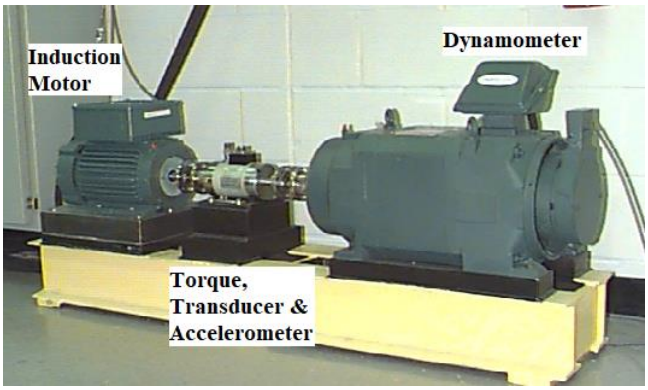

FIGURE 7. Experimental setup of the bearing fault test rig.

FIGURE 8. Three fault conditions: (a) inner race, (b) ball and (c) outer race fault.

Considering the above criteria, we proposed a system that combines the NEEEMD algorithm, an SM method to select

the highest mode of NEEEMD and MOMEDA. In this study, we applied NEEEMD to get multiple IMFs and used the SM value to choose the SM having the highest fault information. Following the MOMEDA filter is used to increase the characteristic fault impulses in the chosen SM. The combination of the proposed method is applied to rolling-element bearings. The fault diagnosis system is summarized below and demonstrated in Fig. 6.

Step 1: Decompose the raw vibration signal into a series of IMFs using NEEEMD.

Step 2: Apply the SM method to the IMFs and obtain the most sensitive IMF based on the greatest SM value.

Step 3: Apply MOMEDA to improve the characteristic fault impulses in the chosen IMF.

Step 4: Use the envelope spectrum to detect the characteristic fault impulses.

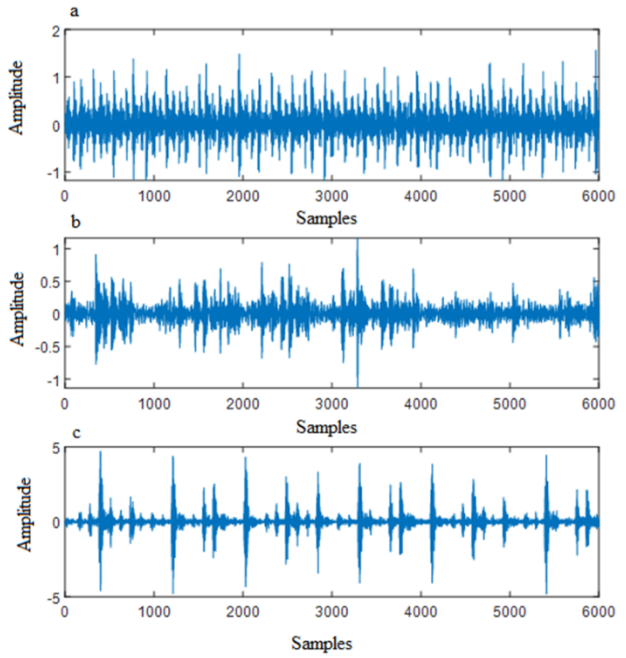

Figure 9. Raw vibration signal obtained from (a) inner race, (b) ball and (c) outer race fault conditions.

IV. Experimental Validation

To validate our proposed NEEEMD method's improved performance in the practical fields of fault diagnosis of rolling elements, the experimental data were obtained from the online dataset of the Case Western Reserve University Bearing Data Center [40] and the experimental setup is showed in Fig. 7. Acceleration data was measured from a 2 hp reliance electric motor bearings. Drive end data is taken from bearing model SKF 6205-2RS JEM. Accelerometers were placed at the 12 o'clock position on the drive end of the motor housing. The sampling frequency is 12 KHz. The rotor shaft's rotating speed is considered, i.e., 1797, 1772 and 1730 rpm and the motor loads are 0 hp, 1 hp and 3 hp, respectively. Speed and horsepower data were collected using the torque transducer/encoder and were recorded by hand. Collected vibration signals include the following operating conditions: (1) inner race fault, (2) ball fault, and (3) outer race fault. Each fault condition includes three different fault sizes, 0.007, 0.014, and 0.021 inches, respectively. The purpose of using different load conditions and rotating speed is to show that the proposed model can obtain the desired output for varying loads and speeds. A visual representation of the fault occurrence in the specific region is illustrated in Fig. 8. The raw vibration signal of 6000 data points from each fault condition is plotted in Fig. 9.

Fig. 9(a) shows that the noise signal is invasive throughout the signal for the inner race condition. It is hard to identify the fault-induced impulses among the heavy noise signal. In Fig. 9(b) ball fault vibration signal was presented. Here the signal has some heavy impulses, making it hard to distinguish between noise and characteristics fault frequency. Fig. 9(c) shows that the noise is not ubiquitous with high amplitude; however, some noise with high amplitude can be seen along with the fault characteristic pulses. This makes it a challenge to differentiate the distinct fault impulses from the noise amplitude. So, the raw signals should be analyzed further with the decomposition methods and some frequency domain plotting is necessary to detect the fault frequency impulses.

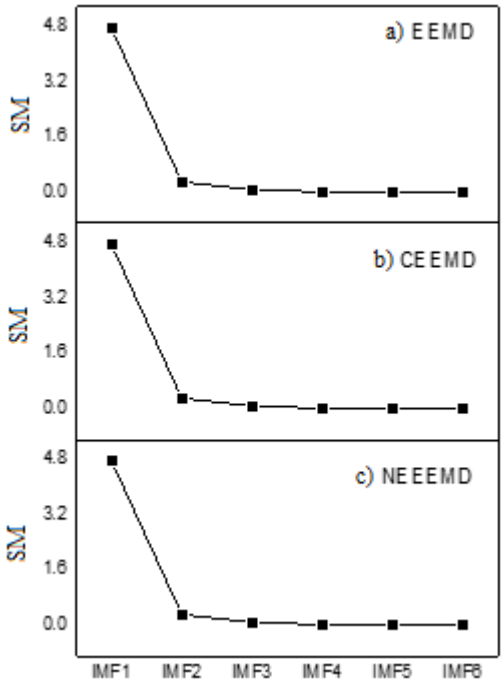

FIGURE 10. SM selection using the proposed method for inner race fault from (a) EEMD, (b) CEEMD, (c) NEEEMD.

The characteristics frequency for each fault condition is obtained from Table 2 [41]. The fault frequency is obtained by multiplying the fault characteristics frequency with the rotor shaft speed. The inner race, ball fault and outer race fault are labelled as case 1, case 2 and case 3, respectively.

The rotating frequency for the cases are 29.95 Hz, 29.53 Hz and 28.83 Hz, whereas the Characteristics frequency are 5.415, 4.714, 3.585, respectively. Multiplying these values, the fault frequency is obtained as 162.179 Hz, 139.204 Hz and 103.368 Hz, respectively.

A. Case 1

The proposed method is used to analyze the vibration signal emanating from the inner race fault in this section. The rotor shaft speed is 1797 rpm and motor load is 0 hp, the diameter of the fault is 0.007" and the characteristics ball pass frequency of the inner race (BPFI) is 162.179 Hz. The first step is to identify the most sensitive mode from different decomposition methods applied to the raw signal. The output of the proposed SP selection method is presented in Fig. 10. From all three methods, it is observed that IMF1 has the highest SM value which is way higher than the following IMFs. So, for EEMD, CEEMD and NEEEMD, IMF1 is selected as the most sensitive case. In Fig. 11, the first IMF obtained from the decomposition methods is plotted. In IMF1 of EEMD and CEEMD, the signal contains huge noise and side-band frequency. On the other hand, the filtered IMF using MOMEDA of NEEEMD can significantly eliminate noise and side-band frequency. Here, the length of filter MOMEDA was 20. The signals are yet to be analyzed to visualize the fault-related impulses distinctively.

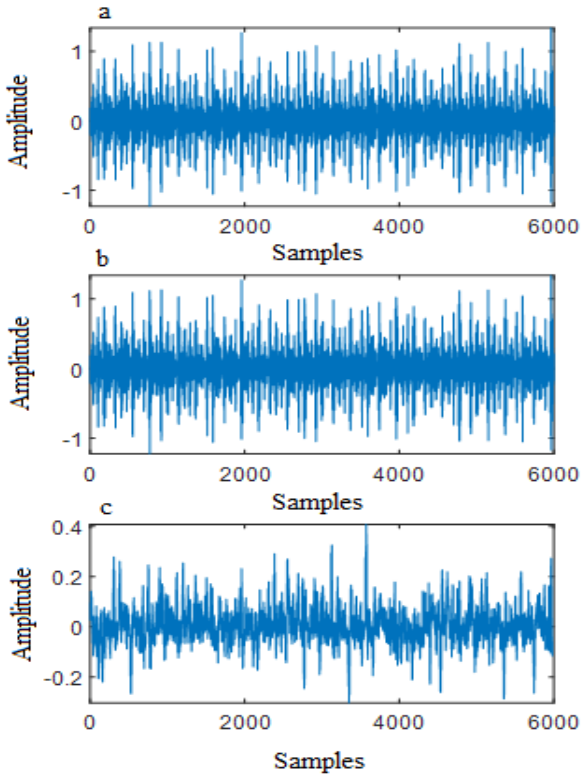

FIGURE 11. Most sensitive mode (IMF1) from (a) EEMD, (b) CEEMD, (c) NEEEMD+MOMEDA, for inner race fault.

Now the selected modes are used to plot the envelope spectrum to analyze the fault characteristics frequency. Fig. 12 shows that the envelope spectrum of EEMD and CEEMD exhibit almost similar characteristics. In both figures, the rotor shaft frequency is evident till the third-order then the fault characteristics till the second order. For NEEEMD the shaft frequency is evident till the third order; however, the fault characteristics till the fifth-order can be identified. So, it can be concluded that the proposed method performed more excellently than the EEMD and CEEMD methods for BPFI identification.

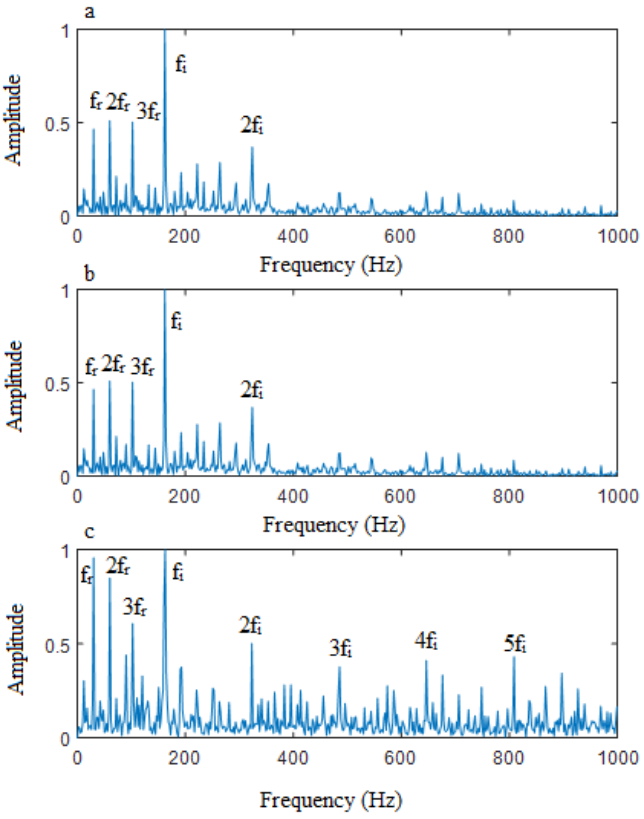

FIGURE 12. Inner race fault diagnosis by envelope signal analysis using (a) EEMD, (b) CEEMD, (c) NEEEMD+MOMEDA.

B. Case 2

In case 2, ball bearing fault was considered where the rotor shaft speed is 1772 rpm and motor load is 1 hp, diameter of the fault is 0.014" and the characteristics ball spin frequency (BSF) is 139.204 Hz. As usual first the most sensitive mode selection was applied to identify the SM from different decomposition methods. Fig. 13 of SM selection shows that in EEMD, CEEMD and NEEEMD, the first IMF is the most sensitive one. Fig. 14 shows the first IMF obtained from the decomposition methods is plotted along with the filtered signal from NEEEMD. Here, the filter length of MOMEDA was set as 20. From the plot, it is observed that there is hardly any visible difference between EEMD and CEEMD. However, for NEEEMD, although the signal seems to contain more noise, some fault impulses with increases amplitude are present. The reason of having more noise

impulses is that the MOMEDA algorithm tries to amplify the fault impulses. Since its an adaptive method, in the process, it also amplifies some of the noise side-bands. However, since we apply envelope spectrum analysis for fault impulses detection, the difference between fault impulses and noise impulses becomes more visible in there.

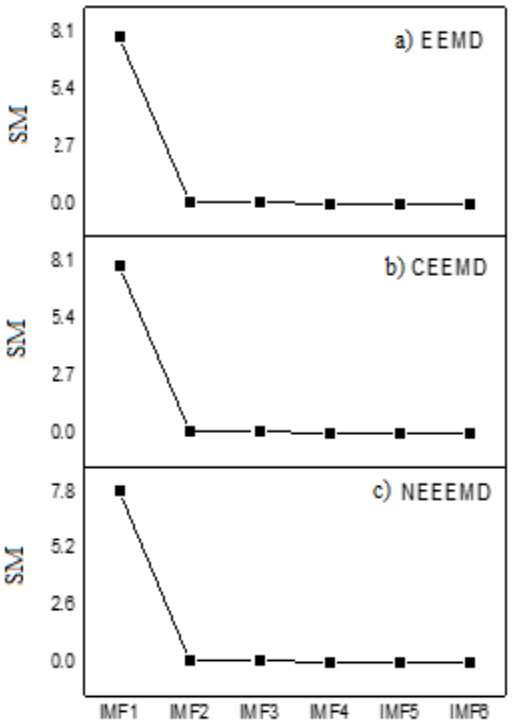

Figure 13. SM selection using the proposed method for ball fault from (a) EEMD, (b) CEEMD, (c) NEEEMD.

Now the selected modes are used to plot the envelope spectrum to analyze the fault characteristics frequency. From Fig. 15, it is observed that the envelope spectrum of EEMD and CEEMD exhibit almost similar characteristics. In all three figures, the rotor shaft frequency is lost amongst the side-bands. Only the first BSF is evident in the envelope spectrum of EEMD and CEEMD. However, although the second and third-order BSF is lost among the noise in the envelope spectrum of NEEEMD, the fourth and fifth-order can be identified. This indicates the superiority of our proposed method.

C. Case 3

In case 3, the outer race bearing fault was considered where the rotor shaft speed is 1730 rpm and motor load is 3 hp, the diameter of the fault is 0.021" and the characteristics ball pass frequency of the outer race (BPFO) is 103.368 Hz. Following the trend, the most sensitive mode selection was first applied to identify the SP from different decomposition methods. Fig. 16 of SM selection shows that in EEMD, CEEMD and NEEEMD, the first IMF is the most sensitive one. After choosing the IMF1 as the SP, the IMF1 obtained from NEEEMD is filtered through MOMEDA where a filter length of 15 provided the best output. The IMF1 from EEMD and CEEMD with the filtered signal of NEEEMD is plotted in Fig. 17. It can be seen that the modes of EEMD and CEEMD contain a lot of other impulses with the fault characteristics impulses. However, the filtered signal using NEEEMD and MOMEDA successfully eliminated some of the side-bands and noise impulses and depicted the fault frequencies lucidly.

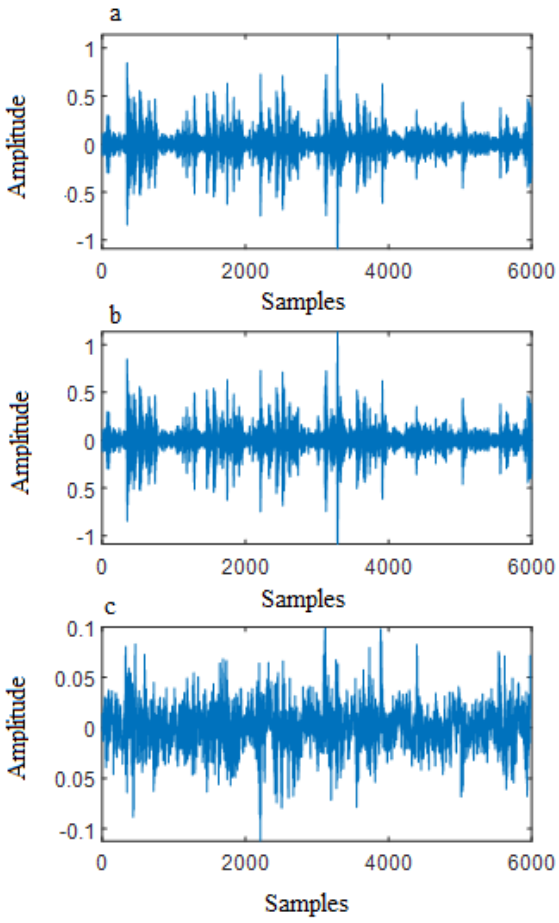

Figure 14. Most sensitive mode (IMF1) from (a) EEMD, (b) CEEMD, (c) NEEEMD+MOMEDA, for ball fault.

Now the selected modes are used to plot the envelope spectrum to analyze the fault characteristics frequency. From Fig. 18, it is observed that, likewise other cases, the envelope spectrum of EEMD and CEEMD exhibit almost similar characteristics. In all three figures, the first order of rotor shaft frequency is evident but later ones are subsided by noise impulses. Envelope spectrum of EEMD and CEEMD can obtain the BPFO till the second-order whereas NEEEMD can conspicuously obtain the 3fo. Moreover, in the envelope spectrum of NEEEMD, the presence of 9fo can be observed.

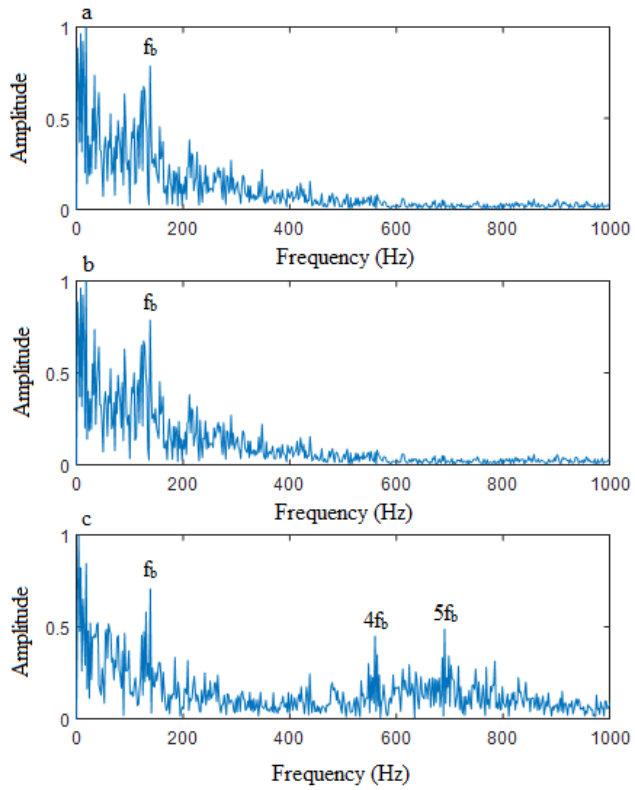

Figure 15. Ball fault diagnosis by envelope signal analysis using (a) EEMD, (b) CEEMD, (c) NEEEMD+MOMEDA.

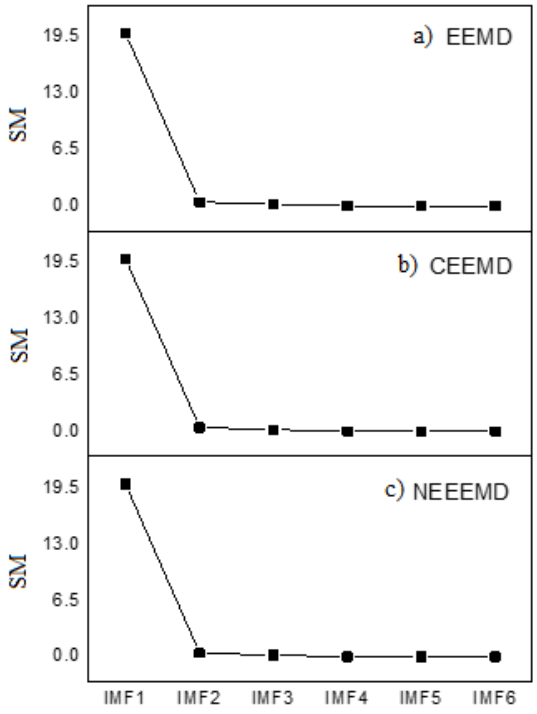

Figure 16. SM selection using the proposed method for outer race fault from (a) EEMD, (b) CEEMD, (c) NEEEMD.

V. CONCLUSION

In this study, a time-frequency adaptive method NEEEMD was proposed to reduce the existing white noise from EEMD. The proposed method was compared with other existing methods, EEMD and CEEMD, on the basis of RRMSE and TESK. In all cases, the proposed method performed better than the other methods which prove that, for the result of RRMSE, our method contains less white noise and for the result of TESK, our method has the most useful information. Later, an SM method was proposed, multiplying energy-entropy in the frequency domain and kurtosis in the time domain to get the SM by considering both time and frequency domain. Further, to enhance the impulse response of fault frequency, the SM is pass through a filter known as MOMEDA. For experimental validation, the proposed method was applied to the bearing dataset. The envelope spectrum of the most SM from EEMD, CEEMD and NEEEMD+MOMEDA were plotted to visualize the fault impulses. Our proposed method (NEEEMD+MOMEDA) had more visual characteristic fault impulses in all the cases and thereby outperformed the existing methods. From the works in this study, we can conclude that:

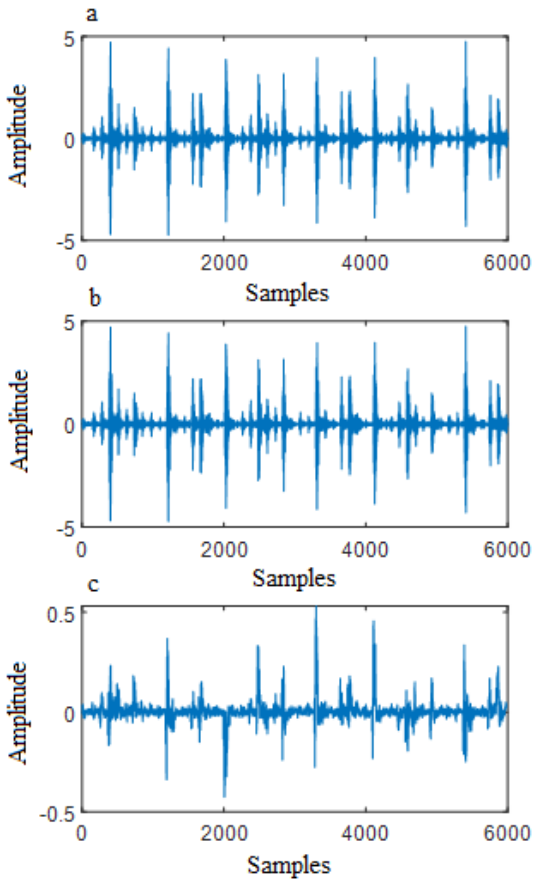

Figure 17. Most sensitive mode (IMF1) from (a) EEMD, (b) CEEMD, (c) NEEEMD+MOMEDA, for outer race fault.

1) Compared to EEMD and its improvement of CEEMD, NEEEMD is more efficient to reduce the presence of white noise.
2) The proposed SM selection method is superior to most other methods used by previous researchers because it considers both time and frequency domain.
3) The MOMEDA filter used with the most sensitive IMF of NEEEMD can effectively obtain more fault-related impulses.

Only the most sensitive mode from all the IMFs was considered to detect the fault impulses in this work. This totally makes sense because the remaining IMFs has less information and may contain useless modes. However, the earlier IMFs still contain some useful fault-related information. In the future stage, the authors aim to select multiple IMFs as required based on the presence of information in their signals. The proposed method will also be compared with other families of the time-frequency adaptive methods to determine universal superiority. Moreover, to generalize the proposed method, other rotating machinery such as gears will be considered.

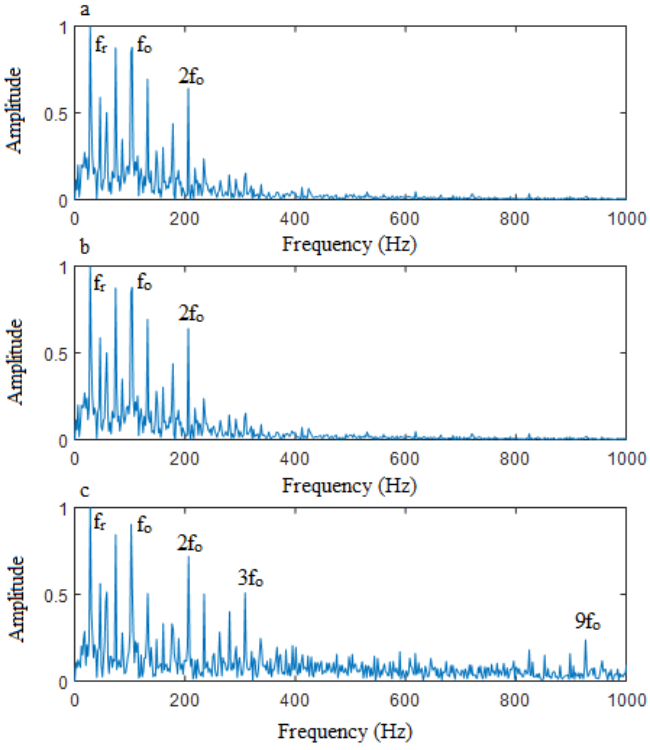

Figure 18. Outer race fault diagnosis by envelope signal analysis using (a) EEMD, (b) CEEMD, (c) NEEEMD+MOMEDA.

ACKNOWLEDGEMENT

The authors are grateful to the Government of Malaysia for the financial support provided under the FRGS/1/2018/TK03/UMP/02/24 grant (RDU190157). The authors also acknowledge the Institute of Postgraduate Studies (IPS), Universiti Malaysia Pahang, for their support through the Master Research Scheme (MRS) scholarship. Additional funding for this research also came from the Institute of Noise and Vibration, Universiti Teknologi Malaysia (RDU192303).

REFERENCES

[1] S. K. Gundewar and P. V. Kane, "Condition Monitoring and Fault Diagnosis of Induction Motor," *Journal of Vibration Engineering and Technologies*, vol. 9, no. 4. Springer, pp. 643–674, Jun. 01, 2021, doi: 10.1007/s42417-020-00253-y.

[2] C. Malla and I. Panigrahi, "Review of Condition Monitoring of Rolling Element Bearing Using Vibration Analysis and Other Techniques," *J. Vib. Eng. Technol.*, vol. 7, no. 4, pp. 407–414, Aug. 2019, doi: 10.1007/s42417-019-00119-y.

[3] X. Chen, S. Wang, B. Qiao, and Q. Chen, "Basic research on machinery fault diagnostics: Past, present, and future trends," *Front. Mech. Eng.*, vol. 13, no. 2, pp. 264–291, 2018, doi: 10.1007/s11465-018-0472-3.

[4] P. Gangsar and R. Tiwari, "Signal based condition monitoring techniques for fault detection and diagnosis of induction motors: A state-of-the-art review," *Mech. Syst. Signal Process.*, vol. 144, p. 106908, 2020, doi: 10.1016/j.ymssp.2020.106908.

[5] H. Feng, R. Chen, and Y. Wang, "Feature extraction for fault diagnosis based on wavelet packet decomposition: An application on linear rolling guide," *Adv. Mech. Eng.*, vol. 10, no. 8, pp. 1–12, 2018, doi: 10.1177/1687814018796367.

[6] H. Keskes, A. Braham, and Z. Lachiri, "Broken rotor bar diagnosis in induction machines through stationary wavelet packet transform and multiclass wavelet SVM," *Electr. Power Syst. Res.*, vol. 97, no. April, pp. 151–157, 2013, doi: 10.1016/j.epsr.2012.12.013.

[7] Q. Zhao, T. Han, D. Jiang, and K. Yin, "Application of Variational Mode Decomposition to Feature Isolation and Diagnosis in a Wind Turbine," *J. Vib. Eng. Technol.*, vol. 7, no. 6, pp. 639–646, Dec. 2019, doi: 10.1007/s42417-019-00156-7.

[8] H. Liu, D. Li, Y. Yuan, S. Zhang, H. Zhao, and W. Deng, "Fault diagnosis for a bearing rolling element using improved VMD and HT," *Appl. Sci.*, vol. 9, no. 7, 2019, doi: 10.3390/app9071439.

[9] J. Cheng, Y. Yang, and Y. Yang, "A rotating machinery fault diagnosis method based on local mean decomposition," *Digit. Signal Process. A Rev. J.*, vol. 22, no. 2, pp. 356–366, 2012, doi: 10.1016/j.dsp.2011.09.008.

[10] . N. H., "Bearing Fault Detection Using Acoustic Emission Signals Analyzed By Empirical Mode Decomposition," *Int. J. Res. Eng. Technol.*, vol. 03, no. 15, pp. 426–431, 2014, doi: 10.15623/ijret.2014.0315084.

[11] A. R. Dash, A. K. Panda, and R. K. Lenka, "Implementation of EMD-based control algorithm for a cascaded multilevel inverter–based shunt active filter," *Int. Trans. Electr. Energy Syst.*, vol. 29, no. 10, p. e12087, Oct. 2019, doi: 10.1002/2050-7038.12087.

[12] T. H. G. Lobato, R. R. da Silva, E. S. da Costa, and A. L. A. Mesquita, "An Integrated Approach to Rotating Machinery Fault Diagnosis Using, EEMD, SVM, and Augmented Data," *J. Vib. Eng. Technol.*, vol. 8, no. 3, pp. 403–408, Jun. 2020, doi: 10.1007/s42417-019-00167-4.

[13] J. Wang, G. Du, Z. Zhu, C. Shen, and Q. He, "Fault diagnosis of rotating machines based on the EMD manifold," *Mech. Syst. Signal Process.*, vol. 135, p. 106443, 2020, doi: 10.1016/j.ymssp.2019.106443.

[14] M. S. P. Reddy, D. M. Reddy, S. Devendiran, and A. T. Mathew,

"Bearing Fault Diagnosis Using Empirical Mode Decomposition, Entropy Based Features and Data Mining Techniques," *Mater. Today Proc.*, vol. 5, no. 5, pp. 11460–11475, 2018, doi: 10.1016/j.matpr.2018.02.114.

[15] A. Zeiler, R. Faltermeier, I. R. Keck, A. M. Tomé, C. G. Puntonet, and E. W. Lang, "Empirical mode decomposition - An introduction," *Proc. Int. Jt. Conf. Neural Networks*, no. July, 2010, doi: 10.1109/IJCNN.2010.5596829.

[16] Q. Xiong, Y. Xu, Y. Peng, W. Zhang, Y. Li, and L. Tang, "Low-speed rolling bearing fault diagnosis based on EMD denoising and parameter estimate with alpha stable distribution," *J. Mech. Sci. Technol.*, vol. 31, no. 4, pp. 1587–1601, Apr. 2017, doi: 10.1007/s12206-017-0306-y.

[17] X. Song, H. Sun, and L. Zhan, "Novel complete ensemble EMD with adaptive noise-based hybrid filtering for rolling bearing fault diagnosis," *J. Vibroengineering*, vol. 21, no. 7, pp. 1845–1858, Nov. 2019, doi: 10.21595/jve.2019.20100.

[18] Z. Wu and N. E. Huang, "Ensemble empirical mode decomposition: A noise-assisted data analysis method," *Adv. Adapt. Data Anal.*, vol. 1, no. 1, pp. 1–41, Jan. 2009, doi: 10.1142/S1793536909000047.

[19] P. Zou, B. Hou, L. Jiang, and Z. Zhang, "Bearing fault diagnosis method based on EEMD and LSTM," *Int. J. Comput. Commun. Control*, vol. 15, no. 1, p. 15, Feb. 2020, doi: 10.15837/ijccc.2020.1.3780.

[20] H. Li, T. Liu, X. Wu, and Q. Chen, "Application of EEMD and improved frequency band entropy in bearing fault feature extraction," *ISA Trans.*, vol. 88, pp. 170–185, May 2019, doi: 10.1016/j.isatra.2018.12.002.

[21] J. R. Yeh, J. S. Shieh, and N. E. Huang, "Complementary ensemble empirical mode decomposition: A novel noise enhanced data analysis method," *Adv. Adapt. Data Anal.*, vol. 2, no. 2, pp. 135–156, Apr. 2010, doi: 10.1142/S1793536910000422.

[22] L. Yang, Q. Hu, and S. Zhang, "Research on fault feature extraction method of rolling bearing based on improved wavelet threshold and CEEMD," in *Journal of Physics: Conference Series*, Feb. 2020, vol. 1449, no. 1, p. 12003, doi: 10.1088/1742-6596/1449/1/012003.

[23] Y. Lu, R. Xie, and S. Y. Liang, "CEEMD-assisted bearing degradation assessment using tight clustering," *Int. J. Adv. Manuf. Technol.*, vol. 104, no. 1–4, pp. 1259–1267, Sep. 2019, doi: 10.1007/s00170-019-04078-2.

[24] J. Rostami, J. Chen, and P. W. Tse, "A signal processing approach with a smooth empirical mode decomposition to reveal hidden trace of corrosion in highly contaminated guided wave signals for concrete-covered pipes," *Sensors (Switzerland)*, vol. 17, no. 2, Feb. 2017, doi: 10.3390/s17020302.

[25] Q. He, P. Li, and F. Kong, "Rolling bearing localized defect evaluation by multiscale signature via empirical mode decomposition," *J. Vib. Acoust. Trans. ASME*, vol. 134, no. 6, Dec. 2012, doi: 10.1115/1.4006754.

[26] R. Yan and R. X. Gao, "Rotary machine health diagnosis based on empirical mode decomposition," *J. Vib. Acoust. Trans. ASME*, vol. 130, no. 2, Apr. 2008, doi: 10.1115/1.2827360.

[27] Y. Lei and M. J. Zuo, "Fault diagnosis of rotating machinery using an improved HHT based on EEMD and sensitive IMFs," *Meas. Sci. Technol.*, vol. 20, no. 12, p. 125701, Nov. 2009, doi: 10.1088/0957-0233/20/12/125701.

[28] H. Endo and R. B. Randall, "Enhancement of autoregressive model based gear tooth fault detection technique by the use of minimum entropy deconvolution filter," *Mech. Syst. Signal Process.*, vol. 21, no. 2, pp. 906–919, Feb. 2007, doi: 10.1016/j.ymssp.2006.02.005.

[29] G. L. McDonald and Q. Zhao, "Multipoint Optimal Minimum Entropy Deconvolution and Convolution Fix: Application to vibration fault detection," *Mech. Syst. Signal Process.*, vol. 82, pp. 461–477, Jan. 2017, doi: 10.1016/j.ymssp.2016.05.036.

[30] X. Zhu and Y. Wang, "Fault diagnosis of rolling bearings based on the MOMEDA and Teager energy operator," *Zhendong yu Chongji/Journal Vib. Shock*, vol. 37, no. 6, Mar. 2018, doi: 10.13465/j.cnki.jvs.2018.06.017.

[31] Z. Wang, J. Wang, Z. Zhao, W. Wu, J. Zhang, and Y. Kou, "Composite Fault Feature Extraction of Gear Box Based on MKurt-MOMEDA," *Zhendong Ceshi Yu Zhenduan/Journal Vib. Meas. Diagnosis*, vol. 37, no. 4, pp. 830–834, Aug. 2017, doi: 10.16450/j.cnki.issn.1004-6801.2017.04.030.

[32] Y. Cheng, Z. Wang, B. Chen, W. Zhang, and G. Huang, "An improved complementary ensemble empirical mode decomposition with adaptive noise and its application to rolling element bearing fault diagnosis," *ISA Trans.*, vol. 91, pp. 218–234, 2019, doi: 10.1016/j.isatra.2019.01.038.

[33] Z. Wu and N. E. Huang, "Ensemble empirical mode decomposition: A noise-assisted data analysis method," *Adv. Adapt. Data Anal.*, vol. 1, no. 1, pp. 1–41, Jan. 2009, doi: 10.1142/S1793536909000047.

[34] X. Qin, Q. Li, X. Dong, and S. Lv, "The Fault Diagnosis of Rolling Bearing Based on Ensemble Empirical Mode Decomposition and Random Forest," *Shock Vib.*, vol. 2017, 2017, doi: 10.1155/2017/2623081.

[35] M. A. Colominas, G. Schlotthauer, and M. E. Torres, "Improved complete ensemble EMD: A suitable tool for biomedical signal processing," *Biomed. Signal Process. Control*, vol. 14, no. 1, pp. 19–29, Nov. 2014, doi: 10.1016/j.bspc.2014.06.009.

[36] Y. Yu, YuDejie, and C. Junsheng, "A roller bearing fault diagnosis method based on EMD energy entropy and ANN," *J. Sound Vib.*, vol. 294, no. 1–2, pp. 269–277, Jun. 2006, doi: 10.1016/j.jsv.2005.11.002.

[37] Z. Wang *et al.*, "Research and application of improved adaptive MOMEDA fault diagnosis method," *Meas. J. Int. Meas. Confed.*, vol. 140, pp. 63–75, Jul. 2019, doi: 10.1016/j.measurement.2019.03.033.

[38] Y. Miao, M. Zhao, J. Lin, and Y. Lei, "Application of an improved maximum correlated kurtosis deconvolution method for fault diagnosis of rolling element bearings," *Mech. Syst. Signal Process.*, vol. 92, pp. 173–195, Aug. 2017, doi: 10.1016/j.ymssp.2017.01.033.

[39] C. J. Zhou, J. Ma, J. Wu, and Z. Feng, "A parameter adaptive MOMEDA method based on grasshopper optimization algorithm to extract fault features," *Math. Probl. Eng.*, vol. 2019, 2019, doi: 10.1155/2019/7182539.

[40] K. A. Loparo, "Bearing data center," *Case West. Reserv. Univ.*, 2013, Accessed: Jun. 02, 2020. [Online]. Available: https://csegroups.case.edu/bearingdatacenter/home.

[41] W. A. Smith and R. B. Randall, "Rolling element bearing diagnostics using the Case Western Reserve University data: A benchmark study," *Mechanical Systems and Signal Processing*, vol. 64–65. Academic Press, pp. 100–131, Dec. 01, 2015, doi: 10.1016/j.ymssp.2015.04.021.